JOURNAL OF Materials CHEMISTRY

Microporous hybrid compounds: hydrothermal synthesis and characterization of two zinciomethylenediphosphonates with 3D structures, structure determination of their dehydrated forms†

K. Barthelet, C. Merlier, C. Serre, M. Riou-Cavellec, D. Riou* and G. Férey

Institut Lavoisier UMR 8637, Université de Versailles, 45 Av. des Etats-Unis, 78035 Versailles Cedex, France. E-mail: riou@chimie.uvsq.fr

Received 12th September 2001, Accepted 22nd January 2002
First published as an Advance Article on the web 19th February 2002

The $ZnCl_2$–H_2O_3P-CH_2-PO_3H_2–NaOH–H_2O quaternary system was investigated under hydrothermal conditions as a function of pH (48 h; 443 K). $Zn_2(H_2O)\{O_3P\text{-}CH_2\text{-}PO_3\}$ (labelled VSB-3(Zn)) and $NaZn_2(OH)\{O_3P\text{-}CH_2\text{-}PO_3\}\cdot 1.5H_2O$ (labelled MIL-48) are obtained at pH 1 and 9 respectively. Their structures were solved from single crystal X-ray diffraction. $Zn_2(H_2O)\{O_3P\text{-}CH_2\text{-}PO_3\}$, isostructural with Co and Ni analogues previously described, is monoclinic ($C\,2/c$ (n° 15)) with lattice parameters $a = 18.7573(3)$ Å, $b = 8.2803(2)$ Å, $c = 8.9225(1)$ Å, $\beta = 106.815(1)^\circ$, $V = 1326.56(4)$ Å^3, $Z = 8$, $R1(F_o) = 0.0269$ and $wR2(F_o^2) = 0.0704$ for 1735 unique reflections $I \geqslant 2\sigma(I)$. Its thermal evolution first leads to anhydrous $Zn_2\{O_3P\text{-}CH_2\text{-}PO_3\}$ (labelled VSB-4(Zn)) whose structure was refined from XRD powder pattern, then to γ and β zinc diphosphates successively. $NaZn_2(OH)\{O_3P\text{-}CH_2\text{-}PO_3\}\cdot 1.5H_2O$ is monoclinic ($P2_1/c$ (n° 14)) with lattice parameters $a = 8.9929(9)$ Å, $b = 5.5093(6)$ Å, $c = 18.025(2)$ Å, $\beta = 92.376(2)^\circ$, $V = 892.3(2)$ Å^3, $Z = 4$, $R1(F_o) = 0.0700$ and $wR2(F_o^2) = 0.1078$ for 2358 unique reflections $I \geqslant 2\sigma(I)$. Its three-dimensional structure provides a new zeotype with 10-membered channels where the Na^+ cations and the water molecules are encapsulated. The elimination of water provides a new compound, $NaZn_2(OH)\{O_3P\text{-}CH_2\text{-}PO_3\}$ (labelled $MIL\text{-}48_{calc}$), whose structure was refined from XRD powder pattern.

Introduction

The hybrid route is now accepted as a very useful tool leading to template-free microporous structures.[1,2] In these phases, the organic chains are functionalized by at least two chelating groups and give rise to three-dimensional frameworks which exhibit strong iono–covalent linkages with the metals. Furthermore, it was initially thought that the incremental increase of the organic chains could lead to microporous properties. Numerous phases have been discovered so far associating alkyldiphosphonic or alkyldicarboxylic acids with rare-earth elements,[3,4] 3d transition metals[5–8] or metalloids of IIIA (13) column.[9–12] Whatever the nature of the cation and the length of the chain, the porosity of the final compounds is crucially related to the rigidity of the organic linker. (i) The alkyldiphosphonic acid with the shortest organic chain ($n = 1$) provides the more open structures: MIL-2[13] is a vanadio-methylenediphosphonate whose 3D structure exhibits 14-membered windows. (ii) The zinc terephthalate MOF-5[14] described by Yaghi *et al.* exhibits a large pore (diameter ~17 Å) cubic structure built up from tetramers of ZnO_4 tetrahedra linked by the terephthalate anions.

This paper deals with the hydrothermal study of the quaternary system $ZnCl_2$–methylenediphosphonic acid–NaOH–H_2O as a function of pH. Two 3D phases are isolated (i) $Zn_2(H_2O)\{O_3P\text{-}CH_2\text{-}PO_3\}$ isotypic with Co[15] and Ni (labelled VSB-3) analogues,[16] (ii) a zeotype structure formulated $NaZn_2(OH)\{O_3P\text{-}CH_2\text{-}PO_3\}\cdot 1.5H_2O$ or MIL-48 whose tetrahedral framework is characterized by 10-membered channels. The thermal degradation of these two phases has already been studied and the structures of their anhydrous forms determined from X-ray powder data.

Experimental

Syntheses

The system was hydrothermally investigated using a mixture of $ZnCl_2$ (Aldrich, 98%), methylenediphosphonic acid (Aldrich, 98%) and deionized water in the molar ratio 1 : 0.5 : 250. The pH of the medium was adjusted by adding various amounts of a concentrated solution of NaOH. The as-prepared mixtures were sealed in a Parr Teflon lined steel autoclave, then heated at 443 K for 48 hours. Solid and liquid phases were separated by filtration. The solid was washed with water then dried in air at room temperature. $Zn_2(H_2O)\{O_3P\text{-}CH_2\text{-}PO_3\}$ is obtained in acidic medium (pH = 1 without NaOH) in the form of parallelepipedic crystals (Fig. 1a) with a yield close to 25% whereas crystals of $NaZn_2(OH)\{O_3P\text{-}CH_2\text{-}PO_3\}\cdot 1.5H_2O$ (MIL-48) are synthesized in basic conditions (pH = 9) in the form of needles (Fig. 1b) with a yield of ~65% (yields calculated by referring to Zn content).

$Zn_2(H_2O)\{O_3P\text{-}CH_2\text{-}PO_3\}$ and $NaZn_2(OH)\{O_3P\text{-}CH_2\text{-}PO_3\}\cdot 1.5H_2O$ were calcined by heating in a tubular furnace 48 hours at 673 K and 575 K respectively, leading to the anhydrous $Zn_2\{O_3P\text{-}CH_2\text{-}PO_3\}$ (noted VSB-4(Zn)) and $NaZn_2(OH)\{O_3P\text{-}CH_2\text{-}PO_3\}$ (noted $MIL\text{-}48_{calc}$) compounds.

Chemical analysis

Thermogravimetric analyses were performed under O_2 flow with a heating rate of 5° min^{-1} using a TA Instruments TGA2050 apparatus.

Elemental analyses were performed both for VSB-3(Zn) and MIL-48. VSB-3(Zn) contents 4.0% of carbon (theoretical (th.):

†Electronic supplementary information (ESI): final Rietveld plots for MIL-48calc and VSB-4(Zn). See http://www.rsc.org/suppdata/jm/b1/b108301p

 DOI: 10.1039/b108301p

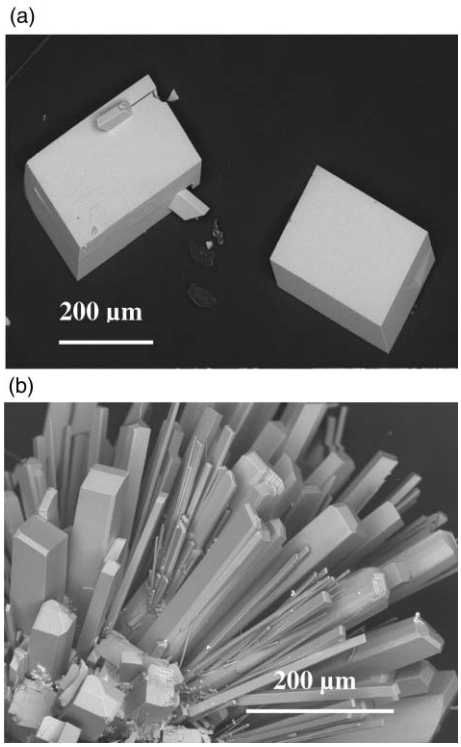

Fig. 1 Scanning electron micrographs of the crystals of $Zn_2(H_2O)\{O_3P\text{-}CH_2\text{-}PO_3\}$ (a) and $NaZn_2(OH)\{O_3P\text{-}CH_2\text{-}PO_3\}\cdot 1.5H_2O$ (MIL-48) (b) (performed with a JEOL SM-5800 LV microscope).

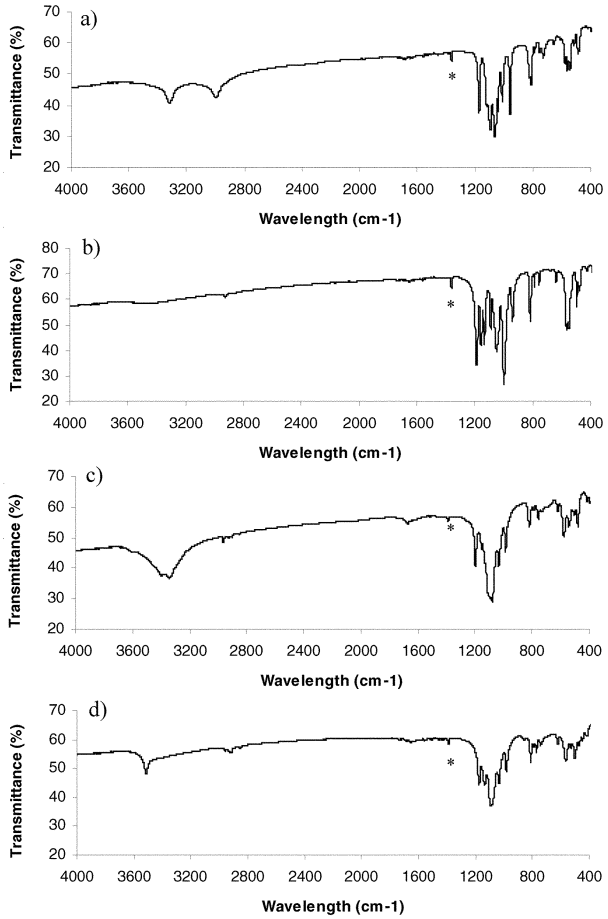

Fig. 2 IR spectra of $Zn_2(H_2O)\{O_3P\text{-}CH_2\text{-}PO_3\}$ (a), $Zn_2\{O_3P\text{-}CH_2\text{-}PO_3\}$ (b), $NaZn_2(OH)\{O_3P\text{-}CH_2\text{-}PO_3\}\cdot 1.5H_2O$ (MIL-48) (c) and $NaZn_2(OH)\{O_3P\text{-}CH_2\text{-}PO_3\}$ ($MIL\text{-}48_{calc}$) (d). (* = impurity).

3.7%), 39.9% of zinc (th.: 40.8%) and 20.9% of phosphorus (th.: 19.3%). For MIL-48, it was found 3.3% of carbon (th.: 3.3%), 16.5% of phosphorus (th.: 16.8%), 6.2% of sodium (th.: 6.2%) and 34.2% of zinc (th.: 35.4%). The efficiency of the dehydration of these two compounds was confirmed both by TG and IR measurements.

The IR spectra (Fig. 2) of the different products crushed in KBr pellets were recorded with a Nicolet Magna-IR 550 in the range 4000–400 cm^{-1}. The methylenediphosphonate groups are characterized by the two small bands at 2900 and 2970 cm^{-1} attributed to CH_2 fragments and by the bands in the range 1000–1200 cm^{-1} due to the P–O and P–C vibrators. Zn–O vibrations appear for lower values around 750 and 820 cm^{-1}. More interestingly, water molecules display bands in the range 3400–3600 cm^{-1}. These bands are sharp in $Zn_2(H_2O)\{O_3P\text{-}CH_2\text{-}PO_3\}$ where the water molecules are linked to Zn metallic centers and disappear in the anhydrous compound. On the other hand, they are broad in MIL-48 due to the disorder of the water molecules inside the channels of the structure. For $MIL\text{-}48_{calc}$, one just observes in this range the sharp signal attributed to the OH vibrators.

Density was measured using a Micromeritics multipycnometer operating under He flow.

X-Ray diffraction‡

The structures of $Zn_2(H_2O)\{O_3P\text{-}CH_2\text{-}PO_3\}$ and $NaZn_2(OH)\{O_3P\text{-}CH_2\text{-}PO_3\}\cdot 1.5H_2O$ (or MIL-48) were solved from single crystal X-ray diffraction. The data were collected at room temperature using a Siemens three-circles diffractometer SMART equipped with a bidimensional CCD detector and working with the monochromatized Mo-Kα radiation (λ = 0.71073 Å). The lattice parameters were determined from a first set of 45 frames then refined during the data collection with all the intensities larger than 10 $\sigma(I)$. The reciprocal spaces were scanned with an ω step of 0.03° and a time per step of 30 seconds, the distance crystal-detector of 4.5 cm allowed a collection up to $2\theta \sim 60°$. Data were reduced with the SAINT program then a semi-empirical absorption correction based on the Blesing method[17] was applied using SADABS program [G. Sheldrick, unpublished]. Both structures were solved applying the direct methods of SHELX-TL.[18] Zn and P atoms were first located then the remaining atoms were deduced from Fourier difference syntheses. H atoms of alkyldiphosphonate groups were found using appropriate geometrical constraints. At the last stage of calculations, all the atoms except H were anisotropically refined.

The X-ray diffraction patterns of $Zn_2\{O_3P\text{-}CH_2\text{-}PO_3\}$ and $NaZn_2(OH)\{O_3P\text{-}CH_2\text{-}PO_3\}\cdot 1.5H_2O$ were recorded with a D5000 Siemens diffractometer using a secondary monochromator and Cu-Kα radiation. The samples were ground in an agate mortar then vertically introduced into a McMurdie sample holder to prevent the preferential orientation effects. The intensities were measured in the range 7–100° (2θ) with a step of 0.02° and a collecting time of 29 s up to 42° (double for the higher values) for VSB-4(Zn) and in the range 8–80° (2θ) with a step of 0.02° and a collecting time of 28 s up to 50° (double for the higher values) for $MIL\text{-}48_{calc}$. The indexations were made using DICVOL91.[19] Monoclinic C-centered and P cells were found with figures of merit $M/F(20)$ = 40/80 (0.0035, 72) and $M/F(20)$ = 50.8/90 (0.0052, 43) for VSB-4(Zn) and $MIL\text{-}48_{calc}$ respectively. The XRD powder patterns were just refined by the Rietveld method using the FULLPROF-2k program integrated in the WinPLOTR software.[20] For VSB-4(Zn), the atomic coordinates of the isostructural VSB-4(Ni)[16] were considered as the starting point.

‡CCDC reference number(s) 174227 and 174228. See http://www.rsc.org/suppdata/jm/b1/b108301p for crystallographic files in .cif or other electronic format.

Table 1 Experimental data collection for $Zn_2(H_2O)\{O_3P\text{-}CH_2\text{-}PO_3\}$ (or VSB-3(Zn)), $Zn_2\{O_3P\text{-}CH_2\text{-}PO_3\}$ (or VSB-4(Zn)), $NaZn_2(OH)\{O_3P\text{-}CH_2\text{-}PO_3\}\cdot 1.5H_2O$ (or MIL-48) and $NaZn_2(OH)\{O_3P\text{-}CH_2\text{-}PO_3\}$ (or $MIL\text{-}48_{calc}$)

$Zn_2(H_2O)\{O_3P\text{-}CH_2\text{-}PO_3\}$	$Zn_2\{O_3P\text{-}CH_2\text{-}PO_3\}$	$NaZn_2(OH)\{O_3P\text{-}CH_2\text{-}PO_3\}\cdot 1.5H_2O$	$NaZn_2(OH)\{O_3P\text{-}CH_2\text{-}PO_3\}$
320.8 g mol^{-1}	302.8 g mol^{-1}	369.8 g mol^{-1}	342.8 g mol^{-1}
Monoclinic	Monoclinic	Monoclinic	Monoclinic
$C\ 2/c$ (n° 15)	$C\ 2/c$ (n° 15)	$P\ 2_1/c$ (n° 14)	$P\ 2_1/c$ (n° 14)
$a = 18.7573(3)$ Å	$a = 18.5380(3)$ Å	$a = 8.9929(9)$ Å	$a = 8.0038(5)$ Å
$b = 8.2803(2)$ Å	$b = 8.1462(2)$ Å	$b = 5.5093(6)$ Å	$b = 5.3092(4)$ Å
$c = 8.9225(1)$ Å	$c = 8.6877(2)$ Å	$c = 18.025(2)$ Å	$c = 17.827(1)$ Å
$\beta = 106.815(1)$ °	$\beta = 106.226(1)$ °	$\beta = 92.376(2)$ °	$\beta = 101.445(2)$ °
$V = 1326.56(4)$ $Å^3$	$V = 1259.71(1)$ $Å^3$	$V = 892.3(2)$ $Å^3$	$V = 742.49(9)$ $Å^3$
$Z = 8$	$Z = 8$	$Z = 4$	$Z = 4$
$\rho_{calc} = 3.214$ g cm^{-3}	$\rho_{calc} = 3.194$ g cm^{-3}	$\rho_{calc} = 2.754$ g cm^{-3}	$\rho_{calc} = 3.068$ g cm^{-3}
$\rho_{meas} = 3.181(6)$ g cm^{-3}	$\rho_{meas} = 3.269(2)$ g cm^{-3}	$\rho_{meas} = 2.74(5)$ g cm^{-3}	$\rho_{meas} = 3.05(1)$ g cm^{-3}
4564 collected data	4651 profile points	5898 collected data	3601 profile points
1735 $I \geqslant 2\sigma(I)$	721 reflections	2358 $I \geqslant 2\sigma(I)$	539 reflections
$R_{int} = 0.030$		$R_{int} = 0.106$	
$R1\ (F_o) = 0.0269$	R_p/R_{wp}: 0.0095/0.1270	$R1\ (F_o) = 0.0700$	R_p/R_{wp}: 0.1380/0.1740
$wR2(F_o^2) = 0.0704$	R_{Bragg}/R_F: 0.0627/0.0454	$wR2(F_o^2) = 0.1078$	R_{Bragg}/R_F: 0.1300/0.0869

The details of data collection are summarized for the four compounds in Table 1. The atomic coordinates are listed in Tables 2, 3, 4, 5 for VSB-3(Zn), VSB-4(Zn), MIL-48 and $MIL\text{-}48_{calc}$ respectively and the main interatomic distances are given in Table 6.

Thermodiffractometric experiments were performed with a D5000 Siemens diffractometer using Co-Kα radiation and equipped with a HTK16 Anton Parr furnace. A small amount of powder was deposited on a Pt strip electrically connected to heating resistances. The XRD patterns (Fig. 3 a–b) were collected under an air atmosphere from room temperature up to 800 °C with a step of 25° and a heating rate identical to the TG experiments.

Table 2 Atomic coordinates ($\times 10^4$) and equivalent isotropic displacement parameters ($Å^2 \times 10^3$) for $Zn_2(H_2O)\{O_3P\text{-}CH_2\text{-}PO_3\}$ (or VSB-3(Zn))

Atoms	x	y	z	U_{eq}
Zn(1)	0	272(1)	7500	9(1)
Zn(2)	−2500	−7500	5000	9(1)
Zn(3)	−1863(1)	−1116(1)	5665(1)	9(1)
P(1)	−1937(1)	−4556(1)	7583(1)	7(1)
P(2)	−935(1)	−1780(1)	9249(1)	7(1)
Ow(1)	−1166(1)	−2250(3)	4612(2)	16(1)
O(2)	−2207(1)	−3300(2)	6283(2)	10(1)
O(3)	−1830(1)	−6217(2)	6970(2)	10(1)
O(4)	−2539(1)	−9544(2)	6373(2)	11(1)
O(5)	−1609(1)	−8815(2)	4716(2)	10(1)
O(6)	−876(1)	−951(2)	7732(2)	11(1)
O(7)	218(1)	1551(3)	9414(2)	12(1)
C	−1034(2)	−3902(3)	8820(3)	11(1)
H(a)	−928(2)	−4486(3)	9803(3)	13
H(b)	−660(2)	−4212(3)	8318(3)	13

Table 3 Atomic coordinates ($\times 10^4$) for $Zn_2\{O_3P\text{-}CH_2\text{-}PO_3\}$ (or VSB-4(Zn))

Atoms	x	y	z
Zn(1)	1916(1)	−1022(3)	4207(3)
Zn(2)	2500	2500	5000
Zn(3)	5000	5358(4)	2500
P(1)	3113(3)	392(6)	2548(7)
P(2)	4097(3)	3176(7)	4245(7)
O(1)	2890(5)	−154(1)	616(1)
O(2)	2558(6)	049(1)	346(1)
O(3)	3188(5)	129(1)	692(1)
O(4)	4830(5)	667(1)	51(1)
O(5)	1610(5)	110(1)	536(1)
O(6)	4130(5)	390(1)	259(1)
C	4050(9)	85(2)	388(2)

Discussion

Structure description and thermal behaviour of $Zn_2(H_2O)\{O_3P\text{-}CH_2\text{-}PO_3\}$

$Zn_2(H_2O)\{O_3P\text{-}CH_2\text{-}PO_3\}$ (or VSB-3(Zn)) presents a three-dimensional framework already encountered with Co[15] and Ni.[16] In the latter case, VSB-3(Ni) results from the condensation by partial dehydration of the VSB-2(Ni) layered structure. Consequently, the VSB-3 structural type keeps in memory this

Table 4 Atomic coordinates ($\times 10^4$) and equivalent isotropic displacement parameters ($Å^2 \times 10^3$) for $NaZn_2(OH)\{O_3P\text{-}CH_2\text{-}PO_3\}\cdot 1.5H_2O$ (MIL-48)

Atoms	x	y	z	U_{eq}
Zn(1)	932(1)	7526(2)	656(1)	16(1)
Zn(2)	3897(1)	227(2)	−2281(1)	16(1)
P(1)	1472(2)	2395(5)	1546(1)	14(1)
P(2)	1687(3)	−964(5)	−984(1)	14(1)
Na	3177(4)	3564(8)	−35(2)	28(1)
O(1)	2008(6)	9950(12)	1253(3)	23(2)
O(2)	3243(6)	−784(12)	−1302(3)	20(2)
O(3)	−1141(7)	8445(12)	749(3)	20(2)
O(4)	1619(7)	4348(11)	960(3)	24(2)
O(5)	5625(7)	2344(12)	−2140(3)	20(2)
O(6)	1720(7)	7250(12)	−338(3)	18(2)
O(7)	2251(7)	1989(12)	−2720(3)	24(2)
C	−468(9)	2098(17)	1716(4)	15(2)
H(a)	−558(9)	1039(17)	2142(4)	19
H(b)	−831(9)	3683(17)	1857(4)	19
Ow(1)	5126(7)	4926(13)	880(3)	28(2)
Ow(2)[a]	4784(104)	−117(231)	132(49)	75(18)

[a]Occupancy = 50%.

Table 5 Atomic coordinates ($\times 10^4$) for $NaZn_2(OH)\{O_3P\text{-}CH_2\text{-}PO_3\}$ (or $MIL\text{-}48_{calc}$)

Atoms	x	y	z
Zn(1)	9497(6)	1822(15)	2057(3)
Zn(2)	3696(5)	7704(18)	343(3)
Na	−275(14)	7350(40)	793(6)
P(1)	1965(12)	2579(28)	926(5)
P(2)	5580(11)	3287(28)	1340(5)
O(1)	9748(20)	7884(32)	1847(8)
O(2)	5563(21)	6073(40)	979(11)
O(3)	2042(26)	4686(40)	396(11)
O(4)	493(20)	2925(64)	1251(9)
O(5)	2024(27)	56(38)	607(15)
O(6)	5710(23)	1819(51)	584(9)
O(7)	7087(17)	3049(58)	2107(9)
C	3632(20)	2711(103)	1797(10)

Table 6 Principal interatomic distances (Å) for $Zn_2(H_2O)\{O_3P\text{-}CH_2\text{-}PO_3\}$ (or VSB-3(Zn)), $Zn_2\{O_3P\text{-}CH_2\text{-}PO_3\}$ (or VSB-4(Zn)), $NaZn_2(OH)\{O_3P\text{-}CH_2\text{-}PO_3\}\cdot 1.5H_2O$ (or MIL-48) and $NaZn_2(OH)\{O_3P\text{-}CH_2\text{-}PO_3\}$ (or $MIL\text{-}48_{calc}$)

VSB-3(Zn)	VSB-4(Zn)	MIL-48	$MIL\text{-}48_{calc}$
Zn(1)–O(7): 1.950(2) (×2)	Zn(3)–O(4): 1.98(1) (×2)	Zn(1)–O(4): 1.929(6)	Zn(1)–O(1): 2.10(2)
O(6): 1.992(2) (×2)	O(6): 2.02(1) (×2)	O(3): 1.946(6)	O(1): 1.83(2)
		O(1): 1.947(6)	O(4): 1.86(2)
		O(6): 1.961(5)	O(7): 2.11(2)
Zn(2)–O(5): 2.070(2) (×2)	Zn(2)–O(3): 2.05(1) (×2)		
O(4): 2.103(2) (×2)	O(5): 2.10(1) (×2)	Zn(2)–O(7): 1.913(6)	Zn(2)–O(2): 1.98(2)
O(3): 2.126(2) (×2)	O(2): 2.13(1) (×2)	O(5): 1.951(6)	O(3): 2.15(2)
		O(5): 1.957(6)	O(5): 1.88(2)
Zn(3)–O(4): 2.041(2)	Zn(1)–O(2): 1.95(2)	O(2): 1.964(6)	O(6): 2.26(2)
Ow(1): 2.045(2)	O(1): 2.14(1)		O(6): 1.92(2)
O(2): 2.049(2)	O(1): 2.05(1)	P(1)–O(7): 1.509(6)	
O(2): 2.132(2)	O(6): 2.12(1)	O(4): 1.518(6)	P(1)–O(3): 1.51(2)
O(5): 2.192(2)	O(5): 2.15(1)	O(1): 1.532(7)	O(4): 1.47(2)
O(6): 2.207(2)		C: 1.791(9)	O(5): 1.47(2)
			C: 1.80(2)
P(1)–O(3): 1.516(2)	P(1)–O(1): 1.49(1)	P(2)–O(6): 1.523(6)	
O(2): 1.531(2)	O(2): 1.47(1)	O(2): 1.537(6)	P(2)–O(2): 1.59(2)
O(4): 1.536(2)	O(3): 1.49(1)	O(3): 1.537(7)	O(6): 1.68(2)
C: 1.816(2)	C: 1.84(2)	C: 1.794(8)	O(7): 1.61(2)
			C: 1.94(2)
P(2)–O(5): 1.523(2)	P(2)–O(4): 1.50(1)	Na–Ow(1): 2.352(7)	
O(7): 1.529(2)	O(5): 1.56(1)	O(4): 2.362(7)	Na–O(1): 2.22(2)
O(6): 1.550(2)	O(6): 1.57(1)	O(3): 2.457(7)	O(3): 2.52(3)
C: 1.797(2)	C: 1.91(2)	O(6): 2.466(7)	O(3): 2.55(2)
		Ow(1): 2.472(7)	O(4): 2.48(4)
		Ow(2): 2.5(1)	O(5): 2.31(3)
		Ow(2): 2.6(1)	O(5): 2.96(3)

2D character and is easily described by the stacking along [100] of hybrid planes joined by one single $Zn(1)O_4$ tetrahedron (Fig. 4a). Inside the planes, Zn(2) and Zn(3) forms along [010] zig-zag chains of edge-sharing octahedra on which tetrahedral methylenediphosphonate units are grafted. Zn(3) displays the particular feature of coordination to five oxygen atoms linked both with another octahedron and a diphosphonate but also to one terminal apex corresponding to a water molecule whose irreversible elimination was followed by TG and thermodiffraction measurements. In the TG curve around 250 °C a weight loss of 4.8% attributed to the dehydration is observed (th. = 5.6%). In the same time the thermodiffractogram (Fig. 3a) shows a structural transformation leading to the anhydrous $Zn_2\{O_3P\text{-}CH_2\text{-}PO_3\}$ compound stable up to 600 °C. The same phase transition has already been described

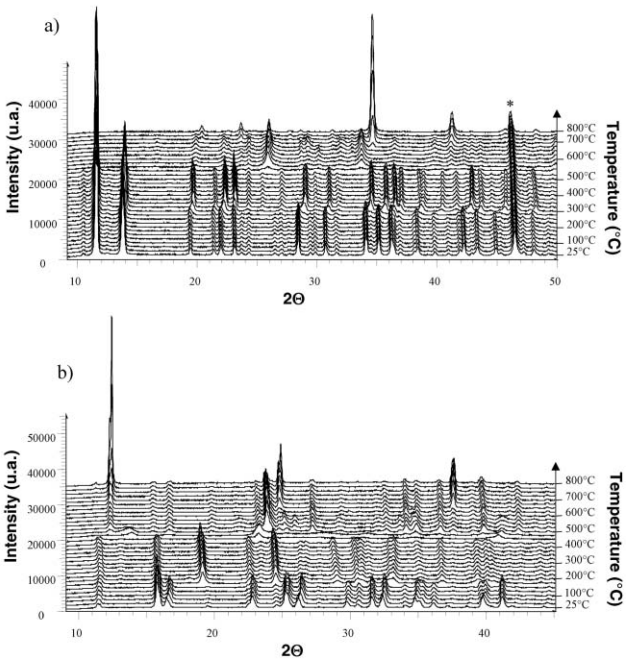

Fig. 3 Thermodiffractograms of $Zn_2(H_2O)\{O_3P\text{-}CH_2\text{-}PO_3\}$ (a) and $NaZn_2(OH)\{O_3P\text{-}CH_2\text{-}PO_3\}\cdot 1.5H_2O$ (b) (* = platinum sample holder).

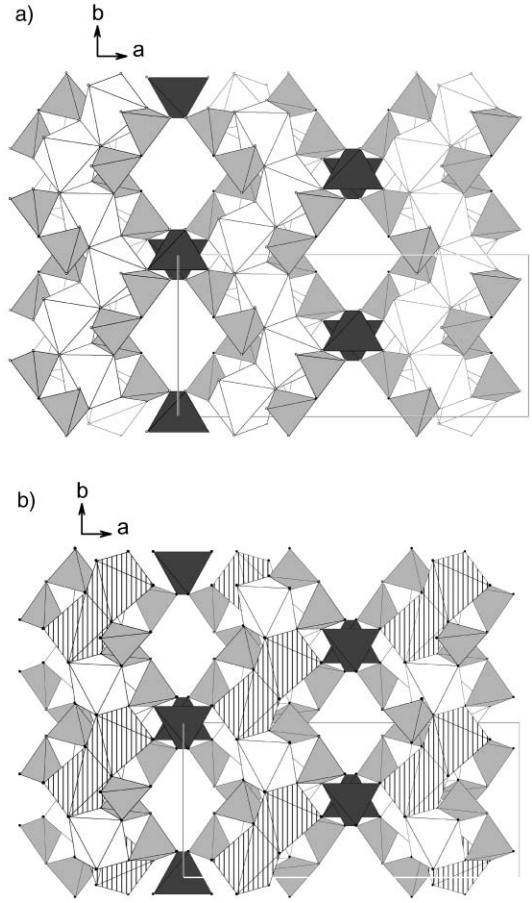

Fig. 4 Projections along [001] of the structures of $Zn_2(H_2O)\{O_3P\text{-}CH_2\text{-}PO_3\}$ (a) and its dehydrated form (b). (Hatching: polyhedra for Zn atoms whose coordination decreases from octahedral in VSB-3(Zn) to square pyramidal in the anhydrous compound).

with Ni replacing Zn. At variance to the Ni system, the monohydrated VSB-3 compounds are directly hydrothermally synthesized with Co and Zn whereas the analogous Ni compound results from the dehydration of the dihydrated lamellar VSB-2 phase. $Zn_2\{O_3P\text{-}CH_2\text{-}PO_3\}$ or VSB-4(Zn) keeps the same polyhedral connections as VSB-3(Zn), just the Zn chains are affected. Indeed, the $ZnO_5(H_2O)$ octahedron becomes a ZnO_5 distorted square pyramid and the zig-zag chains are built up successively from one $Zn(2)O_6$ octahedron and two $Zn(1)O_5$ square pyramids, all edge-shared (Fig. 4b). At temperatures higher than 600 °C, VSB-4(Zn) transforms first into γ-$Zn_2P_2O_7$[21] then into its allotropic β-$Zn_2P_2O_7$ form[22] at 700 °C. Curiously, γ-$Zn_2P_2O_7$ whose structure was determined *ab initio* from X-ray powder diffraction study, is the degradation product at 550 °C of the zinc phenylphosphonate compound $Zn(O_3PC_6H_5)\cdot H_2O$. The transformation from $Zn_2\{O_3P\text{-}CH_2\text{-}PO_3\}$ to γ-$Zn_2P_2O_7$ occurs with a complete rearrangement of the structure even if chemically it just requires the substitution of the bridging CH_2 group of the methylenediphosphonate unit by an equivalent oxygen atom to form a diphosphate moiety. This substitution shows as a small weight increase on the TG curve at 600 °C.

Structure description and thermal behaviour of $NaZn_2(OH)\{O_3P\text{-}CH_2\text{-}PO_3\}\cdot 1.5H_2O$ (MIL-48)

The open structure of $NaZn_2(OH)\{O_3P\text{-}CH_2\text{-}PO_3\}\cdot 1.5H_2O$ or MIL-48 presents two main features. First, its framework is purely zeotypic. Secondly, its three-dimensional structure is built up from the corner-sharing of two types of monodimensional moieties: infinite chains of tetrahedra and columns of hexameric units (Fig. 5). The isolated tetrahedral chains running along [010] (Fig. 6a) are topologically identical to those encountered in the pyroxene type minerals with usual Zn(2)–O distances in the range 1.913(6)–1.964(6) Å (Table 6), they only differ by the bridging atom. Indeed, valence bond calculations[23] show that O(5) corresponds to an hydroxy function leading to $Zn(2)O_2(OH)_2$ tetrahedra *vs.* ZnO_4 tetrahedra in the pyroxene series. The hexamers of the columns (Fig. 6b) contain two $Zn(1)O_4$ tetrahedra and two methylenediphosphonate groups. Within these hexamers, each tetrahedron shares two apices with one diphosphonate group, another one with the other diphosphonate unit of the hexamer and the last one connects the hexamers along [010]. This last apex is up for one tetrahedron of the hexamer and down for the other so

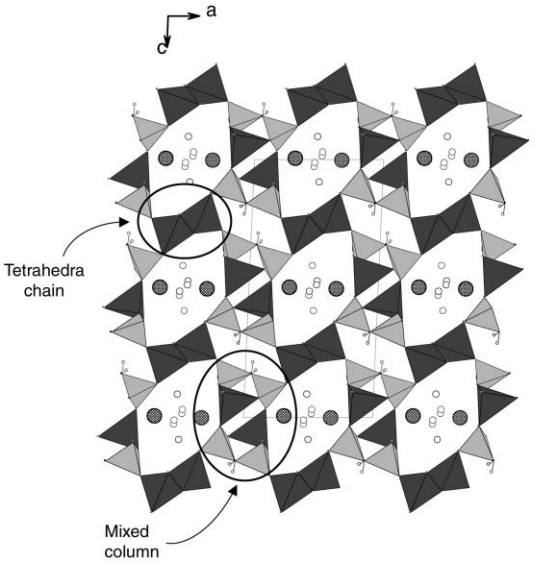

Fig. 5 Projection along [010] of the structure of $NaZn_2(OH)\{O_3P\text{-}CH_2\text{-}PO_3\}\cdot 1.5H_2O$ (MIL-48) showing the 10-membered channels (large and small circles for Na^+ and water molecules respectively).

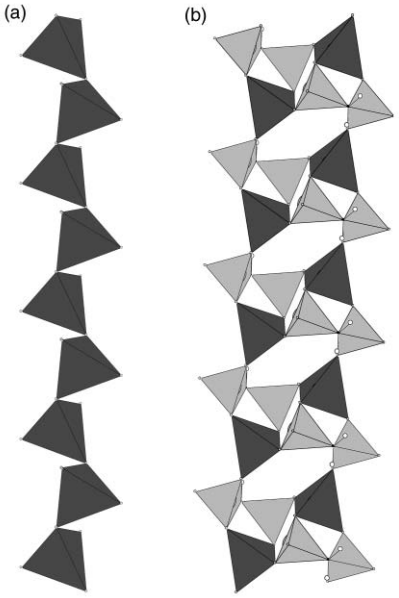

Fig. 6 $NaZn_2(OH)\{O_3P\text{-}CH_2\text{-}PO_3\}\cdot 1.5H_2O$ (MIL-48): one tetrahedral chain (a) and one column built up from corner-sharing hexameric units (b).

leading to columns of corner-shared $Zn(1)O_4$ tetrahedra and methylenediphosphonate groups. It is worth noting that this type of hexameric building block presents some strong structural relationships with the pentamers encountered in the vanadiomethylenediphosphonate compounds[6,24,25] where the two ZnO_4 tetrahedra are replaced by one $V^{IV}O_5$ square pyramid or one elongated $V^{IV}O_5(H_2O)$ octahedron. The basal plane of this octahedron (or square pyramid) is chelated by two methylenediphosphonate units, however, the perpendicular V=O vanadyl linkage prohibits the condensation of the pentamers to create analogous columns as those described in the title compound. The MIL-48 structure is built up from the strict alternation of $Zn(2)O_2(OH)_2$ files and hybrid columns both running along [010] in such a way that their corner-sharing delimit 10-membered tunnels. In these 10-membered tunnels Na^+ cations and water molecules are distributed on two crystallographic sites. TG experiments show that dehydration occurs in two steps with a first weight loss of 3% before 120 °C and a second weight loss of 4.6% in the range 120–200 °C in good agreement with the departures of Ow(2) then Ow(1) (th. 2.4 and 4.8%) (Ow refers to a water molecule). This two-step mechanism seems to be explained by the difference of strengths of interaction between the sodium cations and the two types of water molecules: Ow(1) provides two shorter distances with Na^+ than Ow(2) (Table 6). Thermodiffractometric measurements (Fig. 3b) were performed to study the thermal degradation of MIL-48 up to 800 °C. The irreversible dehydration of MIL-48 leads to $MIL\text{-}48_{calc}$ stable in the temperature range 200–400 °C. At higher temperature, one observes the crystallization of a mixture listed in JCPDS data bank (JCPDS 32-1214) but the structure data remain unknown. The simple elimination of the water molecules from the channels of MIL-48 does not require a complete rearrangement of the framework and $MIL\text{-}48_{calc}$ presents a structure (Fig. 7a) closely related to the initial hydrated phase. The principal changes concern the size of the tunnels and the position of the cations inside them. The tunnels which were occupied both by the water molecules and the sodium cations in MIL-48 are now just filled by the cations. Consequently, the size of the tunnels decreases inducing a diminution of the cell volume ($<15\%$). Furthermore, after the elimination of H_2O from the MIL-48 edifice, coordination of Na^+ cations falls to three and so Na^+ need to move inside the tunnels to complete their coordination

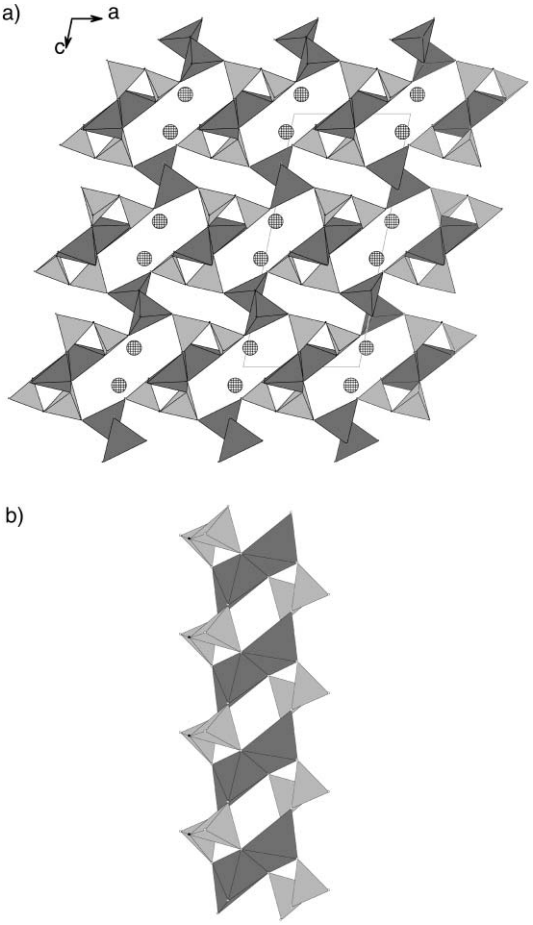

Fig. 7 Projection along [010] of the structure of $NaZn_2(OH)\{O_3P\text{-}CH_2\text{-}PO_3\}$ ($MIL\text{-}48_{calc}$) (a) and one column built up from corner-sharing modified hexameric units (b).

to five (Table 6). This seems also to induce a cooperative transformation of the framework since the ZnO_4 tetrahedra of the hexameric units transform into distorted ZnO_5 square pyramids in such a way that the metallic core of the hexamers become a Zn_2O_8 bipyramid with the two terminal apices of the pyramids pointing up and down the mean plane of the group (Fig. 7b).

References

1 G. Férey, *Chem. Mater.*, 2001, **13**, 3084.
2 B. Chen, M. Eddaoudi, S. T. Hyde, M. O'Keeffe and O. M. Yaghi, *Science*, 2001, **291**, 102.
3 F. Serpaggi and G. Férey, *J. Mater. Chem.*, 1998, **8**, 2737.
4 T. M. Reineke, M. Eddaoudi, D. Moler, M. O'Keeffe and O. M. Yaghi, *J. Am. Chem. Soc.*, 2000, **122**, 4843.
5 P. J. Hagrman, D. Hagrman and J. Zubieta, *Angew. Chem.*, 1999, **38**, 2638.
6 D. Riou, P. Baltazar and G. Férey, *Solid State Sci.*, 2000, **2**, 127.
7 C. Serre and G. Férey, *Inorg. Chem.*, 2001, **40**, 5350.
8 C. Serre and G. Férey, *Inorg. Chem.*, 1999, **38**(23), 5370.
9 K. Maeda, J. Akimoto, Y. Kiyozumi and F. Mizukami, *Angew. Chem.*, 1995, **34**, 1199.
10 L. J. Sawers, V. J. Carter, A. R. Armstrong, P. G. Bruce, P. A. Wright and B. E. Gore, *J. Chem. Soc., Dalton Trans.*, 1996, 3159.
11 H. G. Harvey, S. J. Teat and M. P. Attfield, *J. Mater. Chem.*, 2000, **10**, 2632.
12 C. Paulet, C. Serre, Th. Loiseau, D. Riou and G. Férey, *C. R. Acad. Sci. Ser. IIc: Chim.*, 1999, 631.
13 D. Riou, O. Roubeau and G. Férey, *Microporous Mesoporous Mater.*, 1998, **23**, 23.
14 H. Li, M. Eddaoudi, M. O'Keeffe and O. M. Yaghi, *Nature*, 1999, **402**, 276.
15 D. L. Lohse and S. C. Sevov, *Angew. Chem.*, 1997, **36**, 1619.
16 Q. Gao, N. Guillou, M. Nogues, A. K. Cheetham and G. Férey, *Chem. Mater.*, 1999, **11**, 2937.
17 R. Blesing, *Acta Crystallogr. Sect. A: Found. Crystallogr.*, 1995, **51**, 33.
18 A. Boultif and D. Louer, *J. Appl. Crystallogr.*, 1991, **24**, 987.
19 G. M. Sheldrick, SHELX-TL, version 5.03, Siemens Analytical X-Ray Instrument, Madison, WI, USA (1994).
20 Th. Roisnel and J. Rodriguez-Carjaval, WinPLOTR: a windows tool for powder diffraction patterns analysis, Materials Science Forum, Proceedings of the European Powder Diffraction Conference (EPDIC 7), 2001, vol. 378, p. 118.
21 Th. Bataille, P. Bénard-Rocherullé and D. Louer, *J. Solid State Chem.*, 1998, **140**, 62.
22 C. Calvo, *Can. J. Chem.*, 1965, 1147.
23 N. E. Brese and M. O'Keeffe, *Acta Crystallogr. Sect. B Struct. Sci.*, 1991, **B47**, 192.
24 D. Riou, C. Serre and G. Férey, *Int. J. Inorg. Mater.*, 2000, **2**, 551.
25 G. Bonavia, R. C. Haushalter, C. J. O'Connor and J. Zubieta, *Inorg. Chem.*, 1996, **35**, 5603.